# Fiber orientation effects on high strain rate of Carbon / epoxy composites

**J. F. FERRERO** - I. TAWK** - S. RIVALLANT* - J. J. BARRAU**- M. SUDRE****

*****ENSAE, 10 av. E. Belin 31055 Toulouse / ******LGMT/UPS, 118 rte de Narbonne 31400 Toulouse

E-mail : ferrero@supaero.fr

**Keywords : Carbon Fibre Impact behaviour Mechanical properties Fracture**

**Abstract**

Specific mechanical properties of composites make them particularly attractive. Dynamic loads are of prime interest for their applications. Laminated structures' impact modelling implies prior material dynamic characterisation. This study suggests an analysis of split Hopkinson bar compression testing on T300/914 carbon/epoxy composite material.

First, the effect of fibre orientation and stratification on compression dynamic behaviour is studied. Results show a high non-linearity for +/-45° laminates testing. This non-linearity is not observed when the laminates are reinforced with 0° and 90° plies. Analytical modelling is in agreement with the experimental results. Secondly, experiments are performed on pre-cracked specimens to show the influence of cracking on dynamic behaviour.

## 1. Introduction

Excellent specific properties of composite materials make their use widespread in industrial sectors such as the aerospace's. Structural parts made of composite materials can be subjected during their life to impact damage. Impact modelling requires the knowledge of materials properties for different strain rates. These properties are commonly obtained by split Hopkinson bar testing method. The set-up, originally developed by Kolsky [1], enables an increasing load at high strain rates. The measurements on the bars give the possibility to implement a material law.

Numerous studies have been carried out in order to determine the behaviour of carbon/epoxy and glass/epoxy composite materials both in compression and tension testing. G.H. Staab and A. Gilat [2] have studied the effects of strain rates on glass fibre-epoxy specimens during tensile testing. They have shown that the normal ultimate strength in dynamic tensile testing is superior to the normal ultimate

strength in quasi-static testing. The effect is all the more important as the fibre orientation in the laminate is the smallest. H. Eskandari and J.A. Nemes [3] have found similar results on $[0°/45°/90°/-45°]_s$ carbon fibre-epoxy laminates. The ultimate tensile strength increases with the strain rate. A. Gilat et al. have generalised these results for different stacking sequences of carbon-epoxy laminates [4]. Results obtained in compression testing are similar to the ones obtained in tensile testing [5,6]. H.M. Hsiao et al. [7] have studied the behaviour of carbon fibre-epoxy test specimens for various strain rates and stacking angles: 15°, 30°, 45°, 60 ° and 90°. For 90° specimens, for which the matrix behaviour is prominent, they show an increase of the modulus and of the ultimate load but no significant increase of the deformation. For other orientation specimens, the stress-strain relationship increases with the strain rate. In [8], E. Woldesenbet et al. show the effect of specimen geometry on carbon fibre-epoxy specimens. Jadvah et al. study the effect of strain rates on symmetrical balanced stacking sequences ±15°, ±30°, ±45°… ±90°. The variations with the strain rate strongly depends on fibre orientation. The modulus value is higher than the static value. Delamination and matrix cracking are the principal failure modes.

Tests are performed on ± 45° and ± 30° laminates for which dynamic effects and non-linearities are important. In practice, as for most aeronautical applications, these stacking sequences are seldom used and, if ever they are, the laminates will include 4-directions 0°/45°/90°/-45° laminae. Thus, it is often necessary to withstand secondary loading and to design a stack of plies in regard with repairs and bindings. A major problem in modelling consists in determining whether the analysis shall be carried out at the ply level or at a higher level. In fact, the presence of strong interactions would mean that inverse methods will be used for laminate studies. Furthermore, materials can be subjected to transverse tensile stresses which are major at the time of impact as they can induce microcracks. This is particularly true in structures such as helicopter blades. The dynamic behaviour of such structures is studied here through an analysis of Hopkinson bar compressive tests on carbon fibre-epoxy T300-914 specimens. Tests are performed for different stacking sequences: 0°, ±45°, 90 °, (+45°,90°,-45°) and (+45°,90°,0°,-45°). In addition, tests are performed on precracked specimens in order to analyse the influence of cracking on dynamic behaviour.

## 2. Experimental part

Hopkinson bar principle

The set-up consists of three maraging steel bars (diameter : 20 mm, elastic limit : 1830 Mpa). The first bar or impact bar is propelled into the incoming bar or incident bar by a compressed-gas system. The impactor rate controls the specimen's strain rate. The impact bears a compressive wave in the incident bar. When this compressive wave meets the specimen-bar interface, a part of the wave is reflected whereas the other part is transmitted to the specimen, and then to the output bar or transmitted bar. 350 Ω deformation gauges, located in the middle of the incoming and output bars, measure the wavelengths. The signals are recorded on a digital oscilloscope at a 10 Megahertz sample rate. The set-up is given on Figure I. The bar characteristics are defined in order to check the hypothesis advanced in the theoretical study. Before using the system, some principles given in [9] shall be checked. The bar diameter to the length ratio shall be high enough to get a unidirectional propagation wave. The incident and transmitted bar lengths shall be twice the incident wave length in order to avoid signals superposition. The bars shall be straight and perfectly aligned. To that purpose, they are guided by Teflon rings located on a straight I-beam. The difference between the bar and specimen Poisson's ratios gives rise to friction between the specimen and the bars. Friction can be reduced by lubricating the interfaces.

Data is treated according to the method developed by Gary [10].

The wave equation is written: $\frac{\partial^2 u}{\partial x^2} = \frac{1}{c_b} \cdot \frac{\partial^2 u}{\partial t^2}$ where $c_b$ is the bar wave speed.

The following notation is used: the index i refers to the incident wave, r to the reflected wave and t to the transmitted wave.

The equation solver gives the bar particle velocity as a function of strain.

$$v_i(t) = c_b \cdot \left(\varepsilon_r(t) - \varepsilon_i(t)\right)$$
$$v_t(t) = -c_b \cdot \varepsilon_t(t)$$

It is then possible to get the specimen mean strain rate $\dot{\varepsilon}$ and the specimen mean strain $\varepsilon$ :

$$\dot{\varepsilon}(t) = \frac{v_2(t) - v_1(t)}{L_{ep}}$$

$$\varepsilon(t) = \frac{u_2(t) - u_1(t)}{L_{ep}}$$

where $L_{ep}$ is the specimen length.

The forces in the bars and the specimen mean stress are then given by:

$$F_i(t) = S_b \cdot E_b \cdot \left(\varepsilon_i(t) + \varepsilon_r(t)\right)$$

$$F_r(t) = S_b \cdot E_b \cdot \varepsilon_t(t)$$

$$\sigma_{moy} = \frac{S_b \cdot E_b \cdot \left(\varepsilon_i(t) + \varepsilon_r(t) + \varepsilon_t(t)\right)}{2 \cdot S_{ep}}$$

where $S_{ep}$ is the specimen section, $S_b$ the bar section and $E_b$ the bar Young's modulus.

The bar-specimen set is not unidimensional. As a consequence, the signal measured at the centre of the bar is altered when it comes to the bar-specimen interface. Therefore, it is essential to take into account the scatter between the measurement point and the face where displacements are computed according to Pochemmer and Chree equations in the data treatment.

Specimen definition

Laminates with various stacking sequences are manufactured. The material is T300-914 carbon-epoxy composite material. The polymerisation cycle is performed in an autoclave. Symmetry rules are used for the design of stacking sequences in order to avoid in-plane and out-of-base couplings. Three stacking sequences are used. The first stacking sequence with 0°, 90° and ± 45° laminae is used to characterise the elementary behaviour. The second and third ones, with ± 45° and 90° and with ± 45°, 0° and 90° are used to show the interaction between laminae for the global behaviour.

Specimens are cut according to different orientations and their length is reduced as short as possible in order to eliminate local buckling. The dimensions and the stacking sequences are given on Table II.

## 3. Results and discussion

Static testing

Static compression testing is performed on a mechanical press. Specimens are equipped with strain gages. The force introduced into the specimen is controlled by the machine's pressure transducer .

Figure III shows the different specimens after failure together with the stress-strain curves from the gage measurements. [0°] specimens show a brittle behaviour. The stress-strain relationship is perfectly linear until failure. Failure is of the burst type at 900 MPa.

The stress-strain curve of [90°] specimens is linear until 100 MPa and then slightly deflects. This phenomenon can be interpreted by the control of the resin over the global behaviour. Failure occurs at 180 MPa.

The linear behaviour up to 150 MPa of [± 45°] specimens is followed by a plateau that corresponds to a ply angle variation. This variation is the result of an important resin shear solicitation that normally should not occur on a laminate. Failure occurs at 215 MPa.

Hopkinson bar dynamic testing

Hopkinson bar dynamic testing is performed at specimen strain rates from 100 to 1000 $s^{-1}$, depending on the stacking sequence of the laminate.

Figure IV shows the stress–strain relationships for [90°], [0°] and [±45°] specimens with Hopkinson bar testing. Graph IV.1 presents [90°] specimens stress strain curves for various strain rates. The stress-strain slope is constant for all tests. It means that this is not a strain rate function. This behaviour can be also observed for [0°] and [±45°] specimens. Graphs IV.2 to IV.4 show static and dynamic stress–strain relationships for a given strain rate and for different fiber orientations. The static stress-strain slope is equal to the dynamic stress-strain slope for each stacking sequence.

[0°] specimen dynamic ultimate strength is higher than static ultimate strength. A quasi-linear behaviour is observed until failure. [90°] specimen dynamic ultimate strengh is also superior to the static ultimate strengh. The non-linearity that was observed at 160 MPa for static testing appears approximately at 210 MPa in dynamic testing. [± 45°] specimens stress-strain relationships give identical slopes for static and dynamic testing. However, the non-linearity appears at a higher value, which is due to the resin behaviour.

Figure V show the variations of the ultimate strength with strain rates from 100 to 1000 $s^{-1}$ . Dynamic experimental values are higher than static values whatever the stacking sequence and the strain rate are. However dynamic experimental values do not vary within the tested strain rate.

[± 45°] specimens ultimate strength remains almost constant and equal from 220 to 260 MPa for strain rates from 200 to 960 $s^{-1}$. Nevertheless, the plateau length increases with the strain rate and consequently the ultimate strain is enhanced. [90°] specimens show quasi-linear behaviour up to failure for dynamic testing at strain rates between 180 and 650 $s^{-1}$. This behaviour is controlled by the resin properties.

It is difficult to ascertain that the increase of the ultimate strength is related to dynamic testing or to the testing method. Indeed, compression results are strongly influenced by the specimen shape and size and by the limit conditions. Thus, the small specimen dimensions will lead to important bidimensional stress fields.

Stress-strain relationships are compared for 4 different types of specimen on Figure VI :

[90°] and [± 45°] are the reference stacking sequences and give the ply behaviour

[+45/90/-45] and [+45/90/0/-45] show a complex structure behaviour

Stress-strain relationship for [+45/90/-45] specimens is quasi-linear up to failure.

Results for [+45/90/-45] specimens do not show a plateau as it was observed for [± 45°] specimens for stresses higher than 240 MPa. The [90°] laminae in the stacking sequence do not modify the specimen strength in the longitudinal direction. This means that the behaviour is controlled by the [± 45°] laminae. Furthermore, the computed value by the classical laminate plate theory is equivalent to the experimental value for the linear section of the curve. This result is obtained assuming that the non-linearity observed experimentally in the [± 45°] plies is not computed.

Stresses in compression testing of [± 45°] specimens are such that $\sigma_x \neq 0$ and $\sigma_y = \sigma_z = 0$. It is not true any more when 90° plies are added to the [± 45°] plies as [90°] plies will give rise to strains in the transversal direction. It follows that the [± 45°] plies will not slip and the angle will not change.

A similar behaviour is observed for [+45/90/0/-45] laminates. The presence of [0°] and [90°] plies prevents the non-linear effect observed on [± 45°] plies. This result is very interesting as it explains the difficulties encountered in modelling such stacking sequences. Indeed, the material law used with volume

or multilayer elements fits the law obtained from [± 45°] plies experimental results. If [± 45°] plies are included in a laminate, the material law that is used in the computations must be a linear law corresponding to the laminate law.

In order to estimate the precracking influence on material's dynamic behaviour, [0°] tensile testing is performed on [0°/90°] and [+45°/0°/-45°/90°] specimens. These static tests are carried out at 80% ultimate strength in order to create matrix microcracking in [± 45°] and [90°] plies. The results are displayed on figure VII. Microcracks are apparent on Scanning Electron Microscopy images. Impacts are performed in a direction perpendicular to the crack. Two types of tests are performed: tests up to failure and loaded-unloaded cycles.

Results are presented on figure VIII. They show that the slope of the true stress-strain curve and the ultimate tensile strength are equivalent for plain or precracked specimens. Nevertheless, it does not enable to state on the significance of cracking. Indeed, crack closure during testing can give an explanation to this phenomenon. However, it is not possible to assert whether open cracks behave on the same way. It would require additional Hopkinson bar testing with a precracked specimen under transverse tensile loading.

## 4. Conclusion

Experimental results show different behaviours between static tests and Hopkinson bar tests. A significant increase of the maximal stress is observed for different stacking sequences. However, the true stress-strain curves' modulus remains constant. For specimen strain rates from 200 to 900 $s^{-1}$, there is no significant change of the behaviour. The strong non-linearity observed for [± 45°] specimens corresponds to fibre sliding. This phenomenon disappears in the presence of [90°] and [0°] laminae. These results give the material law used for modelling. Finally, impact on precracked specimens shows that cracking does not influence the specimen response in case of crack closure.

Tests are currently performed to check the validity of the results on other materials (glass/epoxy) and for higher strain rates (> 1000 $s^{-1}$). Furthermore, an experimental set-up is being built for transverse tensile testing.

# Bibliography

[1] Kolsky H. An investigation of the mechanical properties of materials at a very high rates of loading. Proc Phys Soc 1949 ; B-62 ; 676-700 .

[2] Staab G. H., Gilat A., High strain rate response of angle-ply glass – epoxy laminates Vol. 29; No. 10 ; PP 1308-1320 8 Ref 1995.

[3] Eskanderi H., Nems J.A., Dynamic testing of composite laminates with a tensile split Hopkinson bar, Journal of Composite Materials, Vol 34 ,No 4, 2000, pp 260 273

[4] A. Gilat, R. K. Goldberg, G. D. Roberts, Experimental study of strain rate dependent behavior of carbon epoxy composite, Comp. Scien. and Tech., Vol. 62, 2002 pp 1469-1476

[5] B. A. Gama et al, High Strain rate behavior of plain Weave S2 Glass/Vinyl Ester composites, Journal of Composite Materials, Vol. 35, No.13,2001, pp1201-1227

[6] J. R. Vinson, E. Woldesenbet, , Journal of Composite Materials, Vol. 35, No.06,2001, pp509-521

[7] H. M. Hsiao, I.M. Daniel, R.D. Cordes, Strain rate effects on the transverse compressive and shear behavior of unidirectional composites, Journal of Composite Materials, Vol. 33, No.17,1999, pp1620-1642

[8] E. Woldesenbet, J.R. Vinson, Effect of specimen geometry in high strain rate testing of graphite / epoxy composites, Proceedings of the 1997 38$^{th}$ AIAA/ ASME Vol. 2 , Ref. 11, pp 927 – 934, 1997

[9] A. Jadhav, E. Woldesenbet, S.S. Pang, High strain rate properties of balanced angle ply graphite / epoxy composites. Composite : part B, Vol. 34, Ref. 11, pp 339 – 346, 2003

[10] G. Gary, J.R. Klepaczko, H. Zhao, Correction for wave dispersion and analysis of small strains with Split Hopkinson Bar, Proceeding of “International Symposium of Impact Engineering” SENDAI Japan, October 1992.

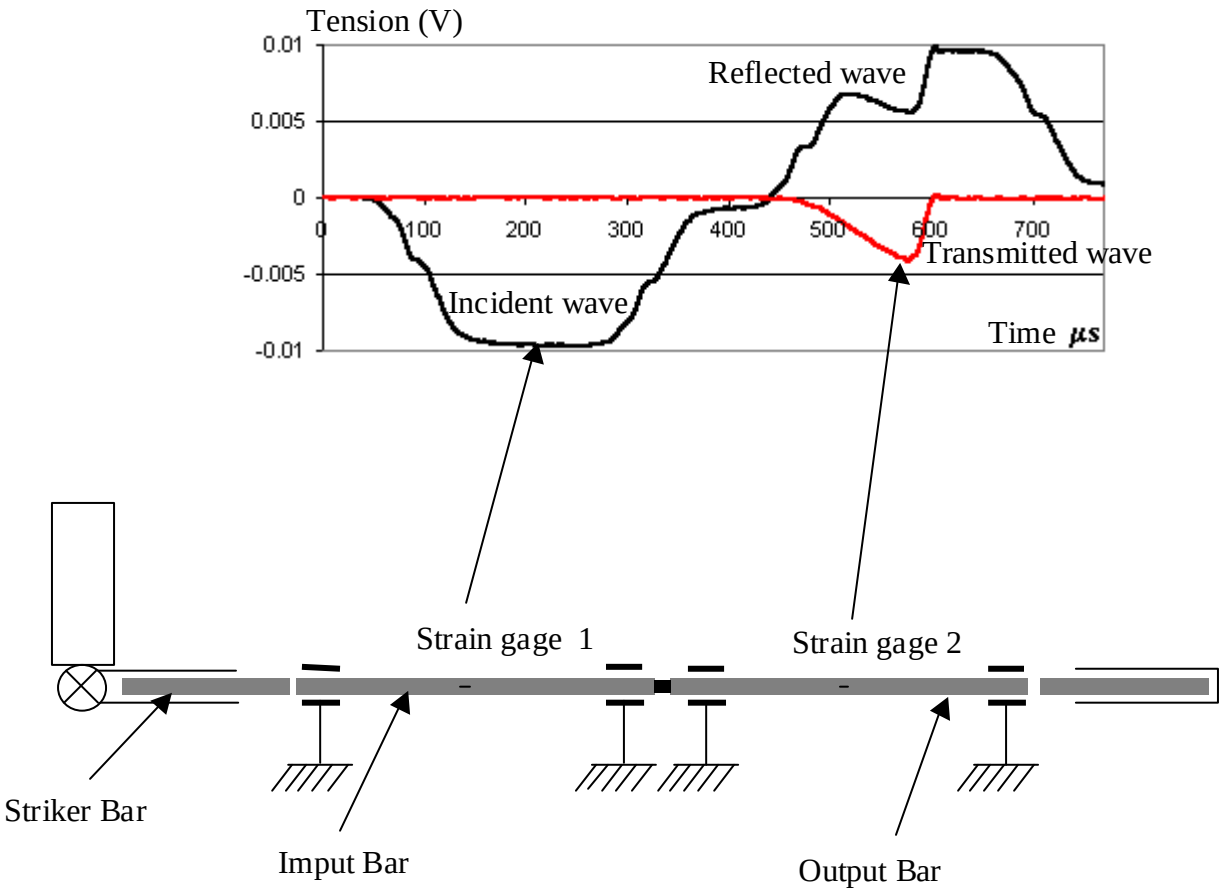


Fig I : Split Hopkinson Pressure Bar : Scheme of experimental set up and Basic recorded signals

Table II : Specimen Definition

| Stacking sequence | Specimen geometry (mm)<br>(Length . width . Thickness) |
|---|---|
| $[(0°)_{30}]$ | 10.15.4 - 15.15.4 - 20.15.4 |
| $[(0°)_{64}]$ | 10.8.8 - 15.8.8 |
| $[(90°)_{45}]$ | 15.15.6 - 20.15.6 |
| $[(90°)_{92}]$ | 10.11.11 - 15.11.11 |
| $[(0° / 90°)_{20}]_s$ | 10.10.5 - 15.10.5 |
| $[(-45° / +45°)_{20}]_s$ | 15.15.5 - 20.15.5 |
| $[(-45° / 90° / +45°)_{15}]_s$ | 15.15.4 - 20.15.4 |
| $[(-45° / 0° / +45° / 90° )_{20}]_s$ | 15.15.5 - 20.15.5 |
| $[(-45° / 0° / +45° / 90° )_{24}]_s$ | 10.10.6 - 15.10.6 |

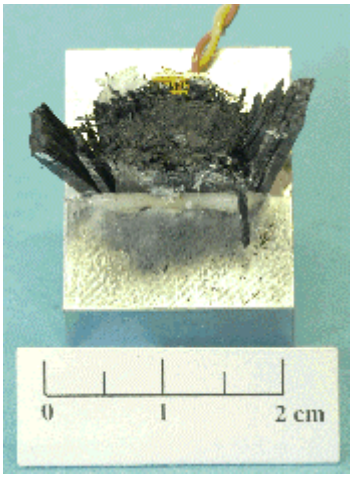


Fiber orientation 0°

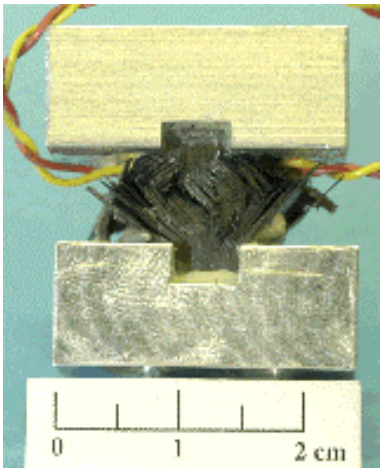


Fiber orientation ± 45 °

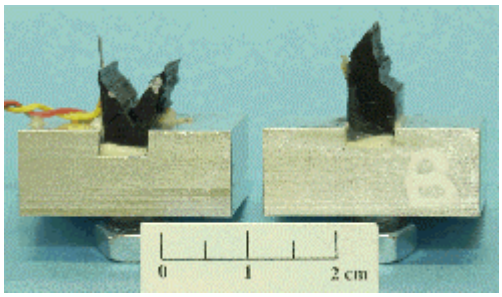


Fiber orientation 90°

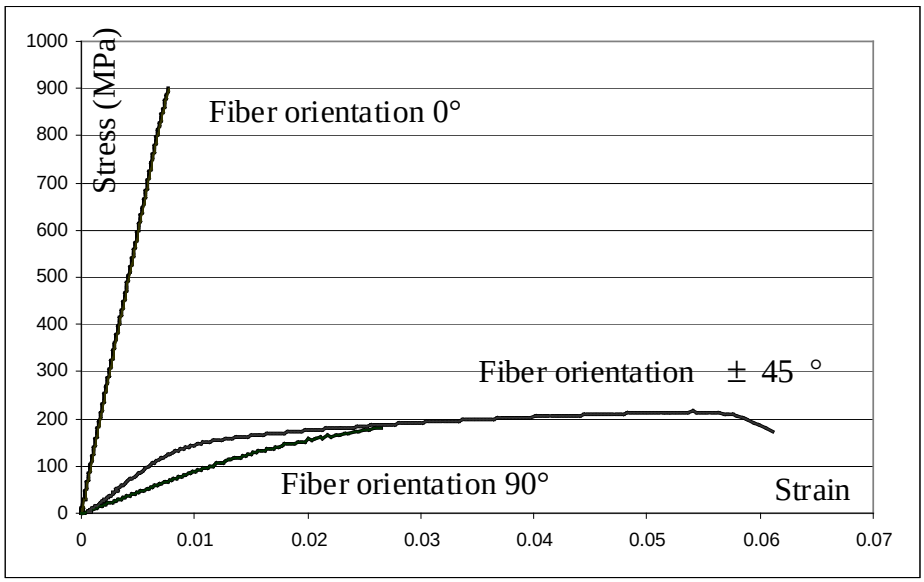


Fig III : Static testing

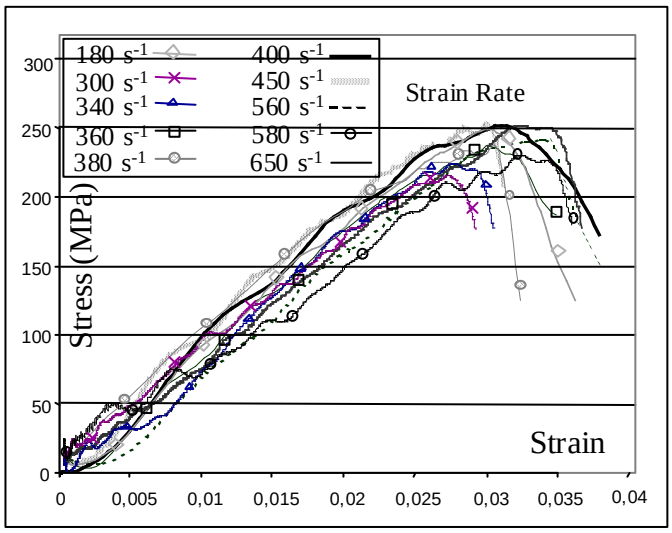


IV.1 Fiber orientation 90°

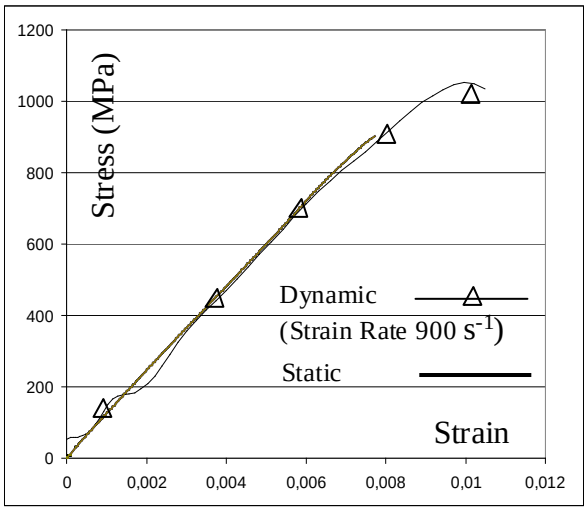


IV.2 Fiber orientation 0°

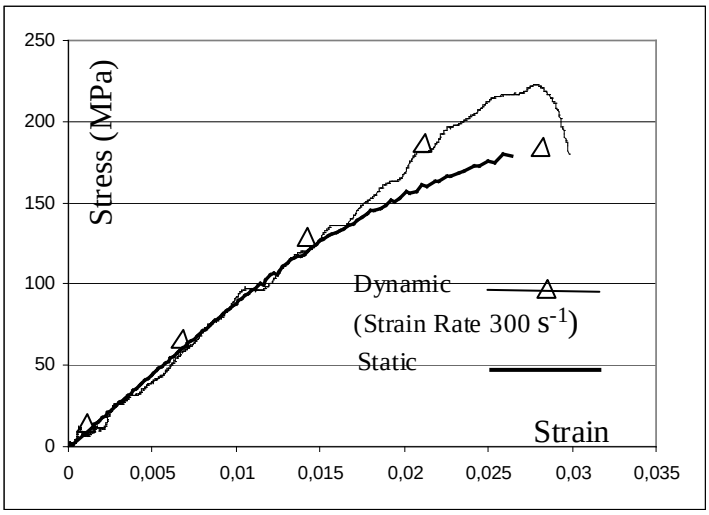


IV.3 Fiber orientation 90°

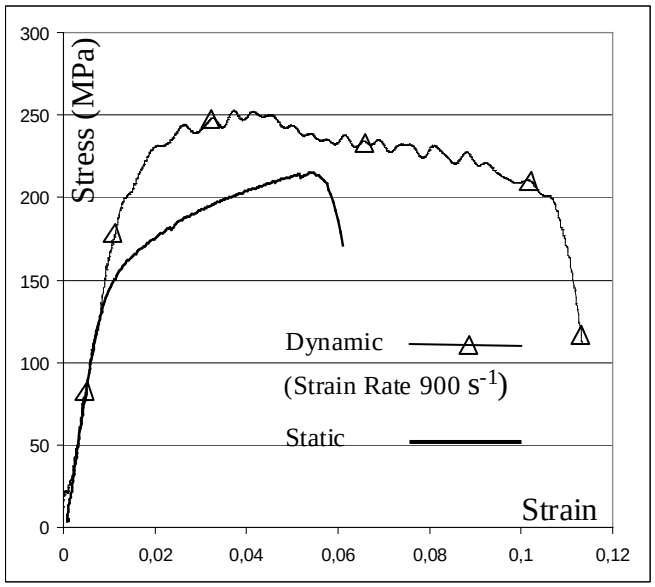


IV.4 Fiber orientation ±45°

Fig. IV : Dynamic testing

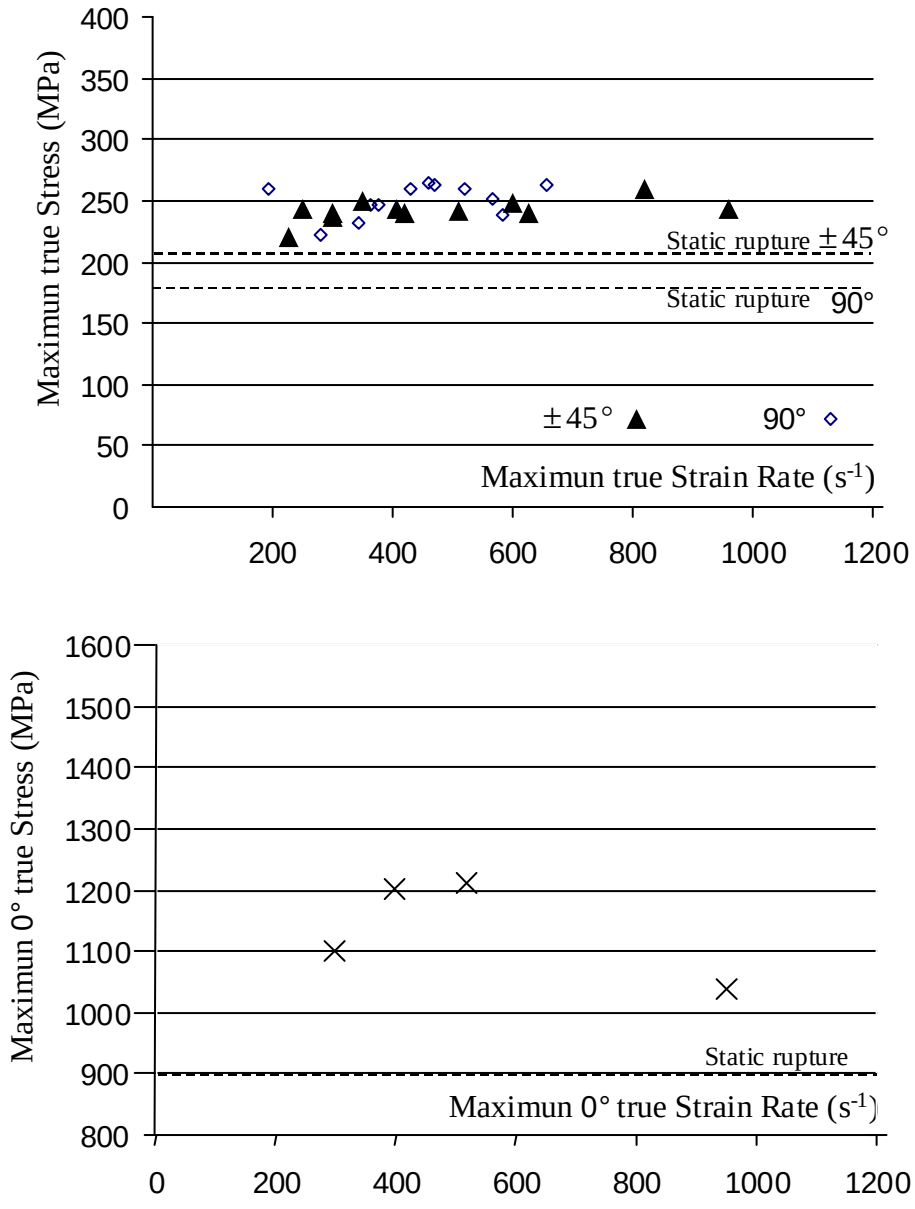


graphe V : Maximun true Stress / Maximun true Strain

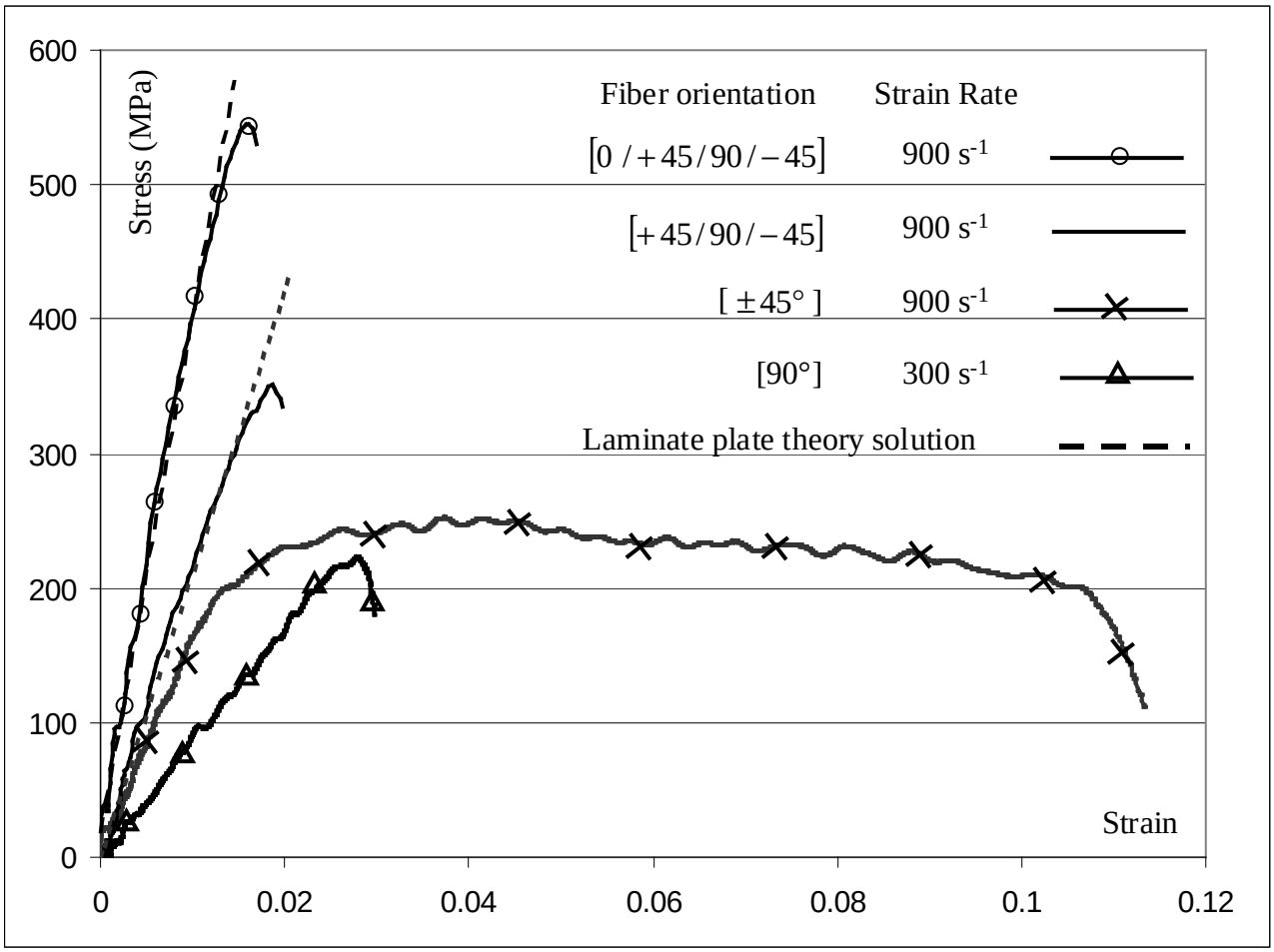


Fig. VI : Dynamics results

Figure VII : microcraking specimen

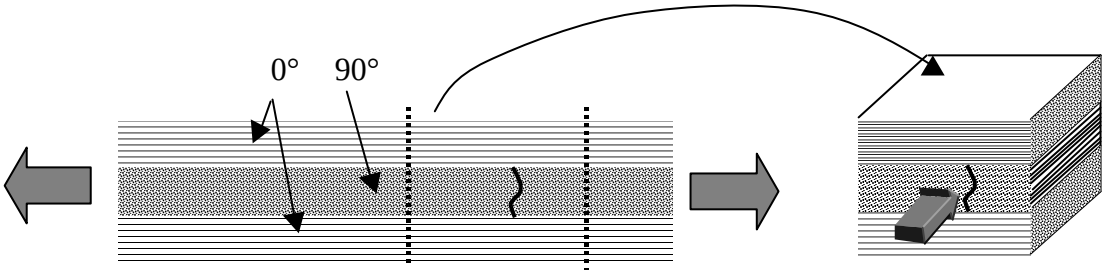


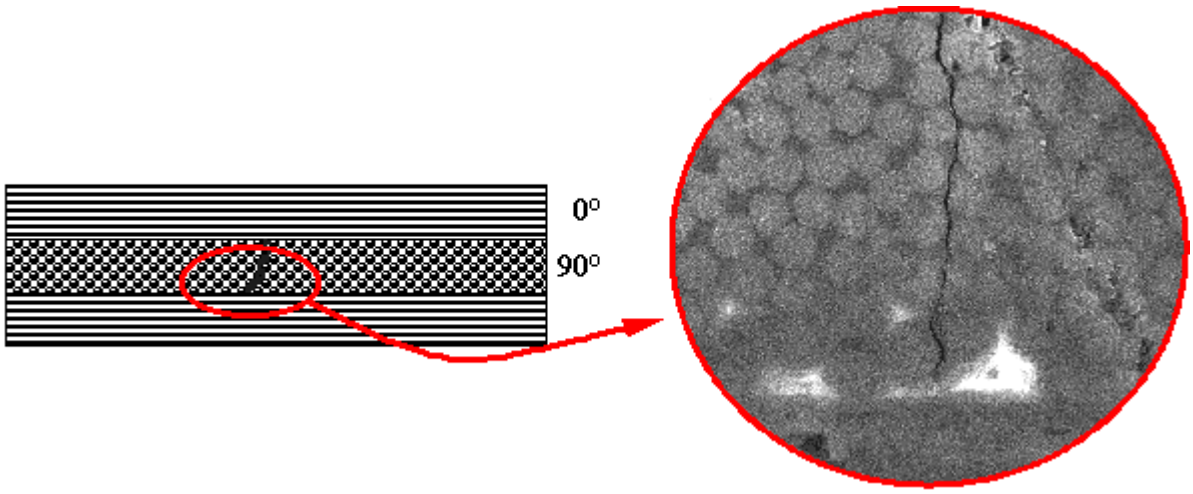


Microcracking in 90° plies

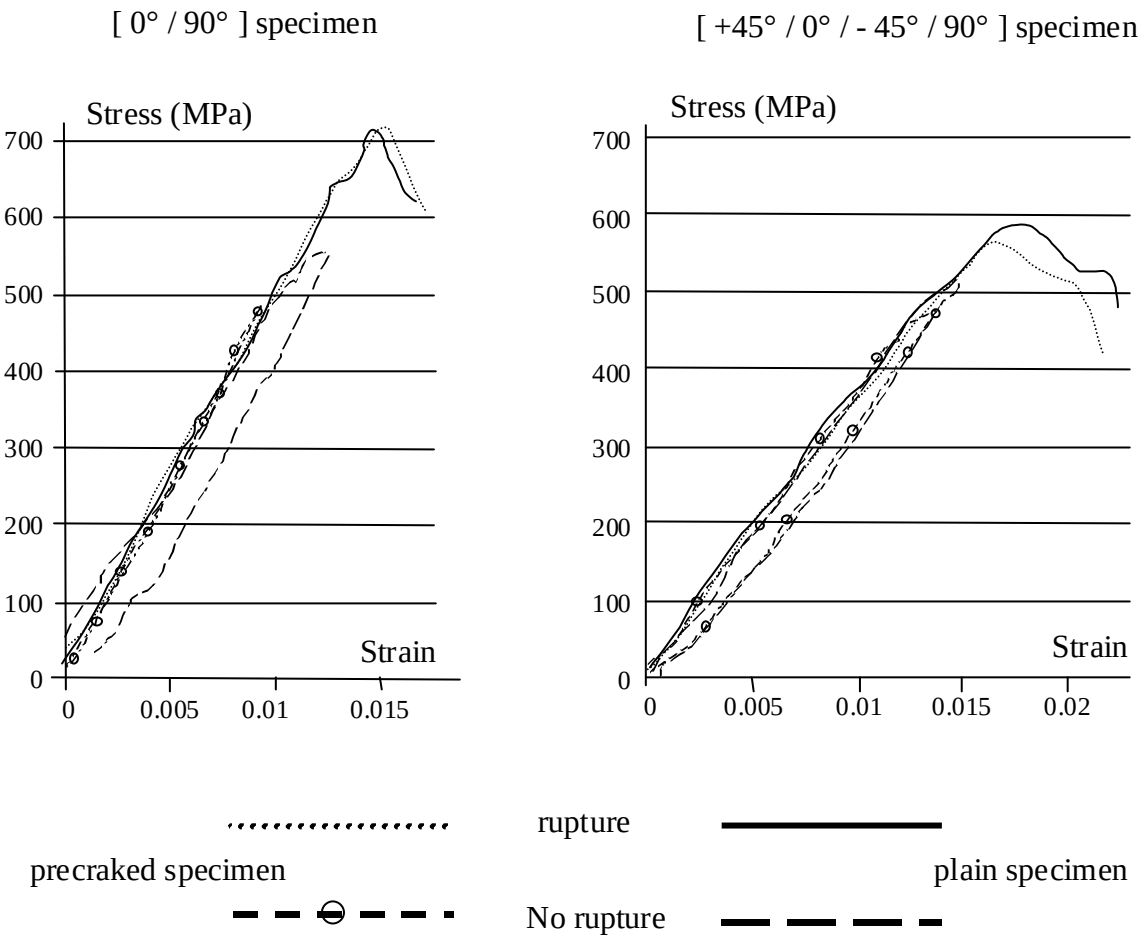


Fig VIII : microcracking specimen dynamic testing